arXiv:1003.3857v1 [cond-mat.mes-hall] 19 Mar 2010

Quantum coherent biomolecular energy transfer with spatially correlated fluctuations

P Nalbach[1], J Eckel[1] and M Thorwart[1,2]

[1]School of Soft Matter Research, Freiburg Institute for Advanced Studies (FRIAS), Albert-Ludwigs-Universität Freiburg, Albertstraße 19, 79104 Freiburg, Germany
[2]I. Institut für Theoretische Physik, Universität Hamburg, Jungiusstraße 9, 20355 Hamburg, Germany

Abstract. We show that the quantum coherent transfer of excitations between biomolecular chromophores is strongly influenced by spatial correlations of the environmental fluctuations. The latter are due either to propagating environmental modes or to local fluctuations with a finite localization length. A simple toy model of a single donor-acceptor pair with spatially separated chromophore sites allows to investigate the influence of these spatial correlations on the quantum coherent excitation transfer. The sound velocity of the solvent determines the wave lengths of the environmental modes, which, in turn, has to be compared to the spatial distance of the chromophore sites. When the wave length exceeds the distance between donor and acceptor site, we find strong suppression of decoherence. In addition, we consider two spatially separated donor-acceptor pairs under the influence of propagating environmental modes. Depending on their wave lengths fixed by the sound velocity of the solvent material, the spatial range of correlations may extend over typical interpair distances, which can lead to an increase of the decohering influence of the solvent. Surprisingly, this effect is counteracted by increasing temperature.

PACS numbers: 03.65.Yz, 71.35.-y, 87.15.ht, 05.60.Gg

Submitted to: *New J. Phys.*

1. Introduction

The photosynthetic conversion of physical energy of sunlight into its chemical form suitable for cellular processes involves many physical and chemical mechanisms [1, 2]. Photosynthesis starts with the absorption of a photon by a light-harvesting pigment forming an exciton, followed by the transfer of the exciton to the reaction center, where charge separation is initiated. It is the nature of this transfer process which is presently in the focus of intense research. Recent experiments [3, 4] provided evidence that an incoherent hopping model seems not to be sufficient to describe long-lasting beating signals in a two-dimensional Fourier transform electronic spectrum [5] recorded from green sulfur bacteria such as *Chlorobium tepidum*. Here, the energy transfer between the

main chlorosome antenna and the reaction centers is mediated by the Fenna-Matthews-Olson (FMO) protein [6, 7, 8] which contains bacteriochlorophyll (BChl) molecules. The FMO protein is a trimer made of identical subunits, each of which contains seven BChl molecules and no carotenoids. Due to its small size, it represents an important model system for photosynthetic energy transfer and has been extensively studied experimentally and theoretically. The observed [3] long lived electronic coherence lasted up to time scales comparable to the time scale of the energy transport. The experiments were performed at low temperature $T = 77$ K and clearly suggest that the exciton moves coherently through the FMO complex rather than by incoherent hopping. Similarly, Lee et al. [4] found coherent beating signals at low temperatures in a two-color electronic coherence photon echo experiment. It allows to directly probe electronic coherences by mixing of the bacteriopheophytin and accessory bacteriochlorophyll excited states in the reaction center of the purple bacterium Rhodobacter sphaeroides. These measurements were performed at 77 K and at 180 K. The coherence beatings in these measurements can only be explained [9] by a strong correlation between protein-induced fluctuations in the transition energies of neighboring chromophores, leading to the conclusion that protein-correlated environments in fact preserve and support electronic coherence in photosynthetic complexes.

Recently, an ultrafast polarization experiment [10] has revealed quantum coherent intrachain (but not interchain) electronic energy transfer in conjugated polymers with different chain conformations as model multichromophoric systems at room temperature. The data suggest that chemical donor-acceptor bonds help to correlate dephasing perturbations. By introducing an angle-resolved coherent optical wave mixing technique, the quantum beating signals between coherently coupled electronic transitions in the light-harvesting complex of purple bacteria are directly observed [11]. Also in the light-harvesting proteins of cryptophyte marine algae, quantum coherent couplings have been identified by exceptionally long-lasting excitation oscillations even at ambient temperature [12].

The consequences of these seminal experiments on long-lived electronic coherences are immediate: the excitation can move rapidly and reversibly in space, allowing for a very efficient search for an energetic minimum in photosynthesis. The subsequent trapping of the excitation, however, must be optimized by properly adjusted environmental fluctuations. In view of potential applications, the recent progress helps to understand the design principle of photosynthetic complexes [13] and to exploit the near-unity efficiency of energy transfer which is believed to result from the constructive interplay of quantum coherence and slow, spatially correlated environmental fluctuations. This could open the door to efficient future artificial light-harvesting complexes finding applications in optimized organic solar cells. The combination of optimized exciton trapping [14] with powerful quantum coherent adaptive control schemes [15, 16, 17] could, in addition, allow to exploit quantum effects to direct the outcome of photochemical processes. Effects beyond the lowest-order Förster treatment, such as the failure of the point-dipole approximation and the

ensuing solvent screening and the sharing of common bath modes have been considered in a generalized Förster theory [18].

Theoretically, photosynthetic energy transfer processes in light-harvesting complexes are often discussed in simplified low-dimensional models describing a few individual chromophores which mutually interact by dipolar couplings and which are exposed to the fluctuations of the polar solvent molecules and the protein host [1, 2, 19, 20, 21, 22, 23]. Two limiting cases are commonly considered: (i) When the dipole coupling between the chromophores is weak in comparison to the coupling of the chromophore to environmental fluctuations, the excitons are considered to be localized at the chromophore sites. The weak electronic coupling can then be treated perturbatively, resulting in an incoherent hopping dynamics described by the standard Förster theory [24]. (ii) In the opposite limit of weak coupling to the environmental fluctuations, standard perturbative quantum master equations are used [25, 26, 27, 28, 29, 30, 31, 32, 33, 34, 35], resulting in a damped coherent dynamics for the exciton transfer. They naturally are based on the Markovian approximation, which renders the time evolution memoryless and allows for a straightforward numerical solution. These types of master equations are appropriate in the case of a clear separation of time scales, i.e., when the time scale on which the environmental fluctuations occur is much smaller than that on which the system dynamics evolves. Formally, this is captured by the requirement that the bath reorganization energy [20] is much larger than the typical system energy. This condition is typically not fulfilled for the energy transfer dynamics in biomolecular light-harvesting complexes in a protein-solvent environment [21, 22, 23, 36]. Here, in addition to the rather slow polarization fluctuations of the polar solvent molecules, the protein cage acts also as a frequency filter which particularly shapes the frequency distribution of the environmental modes. A similar effect arises for electronic spin qubits in semiconductor quantum dots [37] and in donor-based charge qubit crystal systems [38]. Here, the designed geometrical shape of the system structures the acoustic phonon spectrum and gives rise to strong non-Markovian effects. In the context of excitonic energy transfer, it has recently been shown [39, 40, 41] that under realistic biomolecular circumstances, time-local master equations become increasingly unreliable when both time scales become comparable. In addition to the violation of the Markovian assumption, the coupling between chromophores and environment cannot be considered as weak enough to allow for a lowest order perturbative treatment [21, 22, 23]. It was recently shown that the latter condition renders any weak coupling approach questionable [41]. Non-Markovian approaches have been employed beyond a lowest-order treatment [39] and by coupling each chromophore to a single damped harmonic mode [35], whose existence, however, was not further motivated. Alternatively, numerically exact simulations of the real-time dynamics of quantum coherent energy transfer under realistic conditions have been carried out [40, 41, 42] by employing the quasiadiabatic propagator path-integral (QUAPI) [43, 44, 45]. By this, it has been shown that the rather slow polarization fluctuations are one possibility to enhance quantum coherence in the

transfer processes. The coupling of two chromophore pairs to the common slowly fluctuating modes even allows to entangle two excitonic pairs over surprisingly long times even at room temperature [40]. However, when the fluctuations are fast, no entanglement is created even when the two pairs couple to the same modes. The possibility of entanglement and the role of non-Markovian contributions in biomolecular complexes have also been re-addressed in recent works [33, 34, 46]. Slow fluctuations have also been treated [47] by different variants of cumulant expansion techniques and by statistical averaging approaches over static disorder in sum-over-eigenstates approaches. Recently, the standard Redfield equations, which are valid in the weak-coupling regime, have been extended by generalizing the Redfield relaxation tensor on the basis of the Lindblad quantum master equation [48]. This technique goes beyond the secular approximation and thus can include effects of stronger coupling. However, the approach is still memoryless and leads to time-local evolution equations.

Despite the fact that the experimental coherence beatings [9] could only be explained including strong correlations between protein-induced fluctuations in the transition energies of neighboring chromophores, the influence of these correlations received little attention in the theoretical investigations. Nazir [49] investigated the influence of correlated fluctuations on a donor-acceptor system for strong system bath coupling. Correlations in a super-Ohmic bath are found to suppress the crossover to incoherent dynamics at high temperatures, which is in line with the common expectation [20] that a super-Ohmic bath naturally provides only weakened influence of the fluctuations on the system. Similar effects would be expected for correlations in the environment of the chromophores whose spectrum is typically assumed to be Ohmic. Fassiolo et al. [29] discussed the influence of correlations on the trapping probability in a ring of chromophores within a Lindblad master equation approach. They find that the correlations between environmental fluctuations allows to tune the trapping probability.

From a condensed matter point of view, environmental fluctuations are normal modes of the bulk material and thus are typically phonons which propagate through the material. Accordingly they couple to all chromophores with amplitude differences determined by the phase differences due to finite times the modes need to propagate from one chromophore site to the next. However, rattling of side chains of macromolecules in these highly disordered protein environments might well be viewed as a localized excitation. In most existing studies it is assumed that each site of a multichromophoric array is coupled to its local environment. Including in these approaches spatial correlations could be achieved by assuming a finite localization length of the excitations.

In the next section we discuss the influence of spatially correlated environmental fluctuations on a donor-acceptor model using the numerical exact quasi-adiabatic path integral propagator approach which allows us to treat realistic strong couplings and slow environments. Although being a clear oversimplification to realistic exciton transport the donor-acceptor model serves as a toy model to study the influence of spatial correlations and the difference between propagating and localized modes on quantum coherence in detail. In the third section we will discuss how spatial correlations influence

two donor-acceptor pairs which are initially uncoupled. Depending on the distance r_{da} between donor and acceptor and the distance r between the two donor-acceptor pairs spatially correlated fluctuations increase or decrease the decay rates of the coherent dynamics. Finally we discuss and summarize our results.

2. Spatial environmental correlations in a single chromophore pair

2.1. Model

The simplest way to model a single chromophore (or pigment) is by describing it as a quantum two-level system consisting of a ground and an excited state, which are separated by the energy gap ϵ. When the electron is in the excited state, it is localized by its attractive interaction with the hole it left. This dipole electron-hole configuration forms an exciton. A formal description can be given in terms of the Pauli matrix τ_z. Environmental fluctuations will cause transitions between the ground and the excited state and will add a fluctuating energy. Experimentally it is known that the recombination time is of the order of nanoseconds, whereas the complete energy transfer through the complex is of the order of picoseconds. Thus the environmental fluctuations causing recombination are negligible. Describing the fluctuations by harmonic oscillators, which couple linearly to the chromophore, results in the independent boson model for a single chromophore

$$H = \epsilon\frac{\tau_z}{2} - |e\rangle\langle e|\sum_{\mathbf{k}}\lambda_{\mathbf{k}}(\mathbf{r})q_{\mathbf{k}} + \frac{1}{2}\sum_{\mathbf{k}}\left(p_{\mathbf{k}}^2+\omega_{\mathbf{k}}^2q_{\mathbf{k}}^2\right) \tag{1}$$

where we introduced the position and momentum operators, $q_{\mathbf{k}}$ and $p_{\mathbf{k}}$, of the mode with wave vector $\mathbf{k}$ and its coupling $\lambda_{\mathbf{k}}(\mathbf{r})$ to the chromophore which depends on the amplitude of the fluctuation at the position $\mathbf{r}$ of the chromophore. We explicitely coupled the environmental fluctuations only to the excited state, $|e\rangle$, which expresses the fact that the electronic ground state energy is defined by including all vibrational equilibrium energies. We fixed $\hbar = k_B = 1$ which we keep below.

We are not aiming at a complete description of exciton transfer dynamics in complexes like FMO but are merely interested in the question how spatially correlated environmental fluctuations influence the transfer process between two excitonic sites. For the sake of simplicity, we restrict the model under consideration to two chromophore sites (acceptor and donor at $\mathbf{r}_{a/d}$) which contain a single exciton. We do not consider different site energies (i.e., $\epsilon_a = \epsilon_d$) and are thus lead to the donor-acceptor Hamiltonian

$$H_{\rm da} = \frac{1}{2}\Delta\left\{|d\rangle\langle a| + |a\rangle\langle d|\right\} + \sum_{i=a/d}|i\rangle\langle i|\sum_{\mathbf{k}}\lambda_{\mathbf{k}}(\mathbf{r}_i)q_{\mathbf{k}} + \frac{1}{2}\sum_{\mathbf{k}}\left(p_{\mathbf{k}}^2+\omega_{\mathbf{k}}^2q_{\mathbf{k}}^2\right) \tag{2}$$

of a single chromophore pair. The state $|d\rangle$ ($|a\rangle$) denotes the exciton to be at the donor (acceptor) and Δ is the respective dipole coupling matrix element [21].

Comparison of the donor-acceptor model with the spin-boson model

The donor-acceptor Hamiltonian, Eq. (2), can easily be transformed into a Hamiltonian which is closer to the widely studied spin-boson model [19, 20]

$$H_{\rm da} = \Delta\,\frac{\sigma_x}{2} \;+ \frac{\sigma_z}{2}\sum_{\mathbf{k}}\left\{\lambda_{\mathbf{k}}(\mathbf{r}_2) - \lambda_{\mathbf{k}}(\mathbf{r}_1)\right\} q_{\mathbf{k}} \;+ \frac{\mathbb{1}}{2}\sum_{\mathbf{k}}\left\{\lambda_{\mathbf{k}}(\mathbf{r}_2) + \lambda_{\mathbf{k}}(\mathbf{r}_1)\right\} q_{\mathbf{k}} + \frac{1}{2}\sum_{\mathbf{k}}\left(p_{\mathbf{k}}^2 + \omega_{\mathbf{k}}^2 q_{\mathbf{k}}^2\right) \tag{3}$$

by introducing the Pauli matrices $\{\mathbb{1}, \sigma_x, \sigma_y, \sigma_z\}$ with $\sigma_x = |d\rangle\langle a| + |a\rangle\langle d|$ and $\sigma_z = |d\rangle\langle d| - |a\rangle\langle a|$.

One difference is given by the term proportional to $\lambda_{\mathbf{k}}(\mathbf{r}_1) + \lambda_{\mathbf{k}}(\mathbf{r}_2)$ which couples to the identity operator $\mathbb{1}$ of the donor-acceptor system thus causing fluctuations of the reference energy of the donor-acceptor system. Accordingly it is irrelevant for its dynamics. However, this term modifies the bath modes by shifting their zero-point energies and thus changes their thermal equilibrium state. In the spirit of dissipative quantum dynamics, the treatment of system-bath problems typically rely on the assumption that the bath is only weakly influenced by the coupling to the system itself and thus the mentioned effects should not affect the dissipative dynamics of the donor-acceptor system. However, at strong coupling or for a slow bath with cut-off frequency $\omega_c \lesssim \Delta$ the validity of these assumptions is questionable [50]. Thus the dynamics generated by our donor-acceptor Hamiltonian in Eq. (2) differs from the standard spin-boson problem in three aspects. First, the thermal equilibrium state to which the total system is driven is different and, second, the factorized initial conditions for both cases reflect two different initial conditions. Third, in the spin-boson model, a single bath is coupled to the system whereas in the donor-acceptor Hamiltonian, two baths are coupled to the system states. Thus, even when both baths are mutually uncorrelated, the resulting rates for the donor-acceptor system are twice as large compared to the spin-boson model (assuming that all baths are coupled with equal strength). This has to be taken into account when comparing results from both approaches.

2.2. The quasiadiabatic propagator path integral for the multi-bath case

The dynamics of the donor-acceptor is characterized by the time evolution of the reduced density matrix $\rho(t)$, which is obtained after tracing out the environmental (or bath) degrees of freedom, i.e.,

$$\rho(t) \;=\; \mathrm{Tr}\left\{U(t,0)W(0)U^{-1}(t,0)\right\}_B \tag{4}$$

and

$$U(t,0) \;=\; \mathcal{T}\exp\left\{-\frac{i}{\hbar}\int_0^t ds H_{da}\right\}. \tag{5}$$

Here, $U(t,0)$ denotes the propagator of the full system plus bath and $\mathcal{T}$ denotes the time-ordering operator. $W(0)$ is the total density operator at initial time set at $t = 0$. We assume standard factorizing initial conditions [20], i.e. $W(0) \propto \rho(0)\exp(-H_B/T)$,

where the bath with the Hamiltonian $H_B = \frac{1}{2}\sum_k (p_k^2 + \omega_k^2 q_k^2)$ is at thermal equilibrium at temperature T and the system is prepared according to $\rho(0)$. Throughout this work, we always start with the exciton at the donor site, i.e., $\rho(0) = |d\rangle\langle d|$.

We calculate $\rho(t)$ using the numerically exact quasiadiabatic propagator path-integral (QUAPI) [43, 44, 45] scheme. For details of the iterative technique, we refer to previous works [43, 44, 45]. In brief, the algorithm is based on a symmetric Trotter splitting of the short-time propagator $\mathcal{K}(t_{k+1}, t_k)$ for the full Hamiltonian into a part depending on the system Hamiltonian and a part involving the bath and the coupling term. The short-time propagator describes time evolution over a Trotter time slice δt. This splitting is by construction exact in the limit $\delta t \to 0$ but introduces a finite Trotter error for a finite time increment, which has to be eliminated by choosing δt small enough such that convergence is achieved. On the other side, the bath degrees of freedom generate correlations being non-local in time. For any finite temperature, these correlations decay exponentially fast at asymptotic times, thereby setting the associated memory time scale. QUAPI now defines an object called the reduced density tensor, which lives on this memory time window and establishes an iteration scheme in order to extract the time evolution of this object. Within the memory time window, all correlations are included exactly over the finite memory time $\tau_{\rm mem} = K\delta t$ and can safely be neglected for times beyond $\tau_{\rm mem}$. Then, the memory parameter K has to be increased, until convergence is found. The two strategies to achieve convergence are naturally countercurrent, but nevertheless convergent results can be obtained in a wide range of parameters.

For the purpose of this work, we have to extend the standard formulation of QUAPI which only includes the coupling to one bath. The entire influence of a single bath coupled via the operator $\hat{s}$ to the donor-acceptor system is described in terms of the real-time path-integral formulation by the influence functional

$$I(\{s_i^+, s_i^-\}; \delta t) \;=\; \exp\left\{ -\frac{1}{\hbar} \sum_{i=0}^{N} \sum_{i'=0}^{i} \left[s_i^+ - s_i^-\right] \left[\eta_{ii'} s_{i'}^+ - \eta_{ii'}^* s_{i'}^-\right] \right\} \tag{6}$$

where the path segments $s_i^{\pm}$ associated to a Trotter time slice i given as interval $[(i - \frac{1}{2})\delta t, (i + \frac{1}{2})\delta t]$ (with total time $t = N\delta t$) are assumed to have constant values over a single time slice. The number of path segments within a Trotter time slice is given by the dimension of the Hilbert space in which the system-bath coupling operator lives. The superscript $\pm$ denotes the propagation direction forward or backward in time since we work with density operators. The total path integration over all paths $s^{\pm}(t')$ has to be performed as the discrete sum over all configurations $\{s_i^+, s_i^-\}$ of paths segments between initial and final time. The time-discrete bath correlators $\eta_{ii'}$ are defined in Ref. [43] and the superscript * denotes the complex conjugate.

Multiple independent baths, $H_{B\alpha}$, which couple to system operators $\hat{s}_\alpha$ will simply cause a product of influence functionals since each bath acts separately as described

above. Thus, the total influence functional assumes the form

$$I(\{s^+_{i,\alpha}, s^-_{i,\alpha}\}; \delta t) \;=\; \exp\left\{ -\frac{1}{\hbar} \sum_{\alpha} \sum_{i=0}^{N} \sum_{i'=0}^{i} [s^+_{i,\alpha} - s^-_{i,\alpha}] \left[\eta^{(\alpha\alpha)}_{ii'} s^+_{i',\alpha} - \eta^{*(\alpha\alpha)}_{ii'} s^-_{i',\alpha} \right] \right\} \quad (7)$$

Here we denoted the bath correlators $\eta^{(\alpha\alpha)}_{ii'}$ with the additional superscripts since for differing baths the correlators will differ.

The question whether the environmental fluctuations act *locally* or in a correlated manner can be tackled by the following extension. Local fluctuations couple to the donor and to the acceptor separately and independently. This implies that Eq. (7) describes *all* effects due to environmental fluctuations. If, however, the fluctuations are caused by extended waves, like phonon modes or if the fluctuations rattling the donor can at least partially still be felt at the acceptor site, then the fluctuations at the various sites are no longer independent and spatial correlations have to be taken into account. Hence, Eq. (7) has to be generalized to

$$I(\{s^+_{i,\alpha}, s^-_{i,\beta}\}; \delta t) \;=\; \exp\left\{ -\frac{1}{\hbar} \sum_{\alpha,\beta} \sum_{i=0}^{N} \sum_{i'=0}^{i} [s^+_{i,\alpha} - s^-_{i,\alpha}] \left[\eta^{(\alpha\beta)}_{ii'} s^+_{i',\beta} - \eta^{*(\alpha\beta)}_{ii'} s^-_{i',\beta} \right] \right\} \quad (8)$$

where $\eta^{(\alpha\beta)}_{ii'}$ are the mixed bath correlators expressing the correlations of the fluctuations acting at operator $\hat{s}_\alpha$ and $\hat{s}_\beta$. The detailed numerical evaluation of the influence functional in the extended QUAPI scheme becomes more involved, but the general procedure is not affected by this extension.

2.3. Correlated environmental fluctuations at different sites

In a crystal, environmental fluctuations acting, e.g., on electrons, are generated by vibrations of the lattice atoms and are the well-known phonons. Phonons are also present in disordered media (condensed, soft or fluid). In the sense of propagating modes of the host material which evolve with time through the medium, they are commonly limited to the low energy sector or, more specifically, to energies associated to wave lengths on which the material appears homogeneous. Once the wave length becomes smaller than the disorder length scale, the modes can generally be thought of as localized fluctuations. However, their localization length (or radius) is still connected to the wave length of the mode and accordingly even a *localized* mode extends over some finite spatial range. The same picture holds for dipolar fluctuations in solvents and vibrations of charged macromolecular side chains forming the bio-environment of light harvesting complexes. Excitons, as coupled electron hole pairs, have an electric dipole moment $\vec{\mu}$ which couples to the electric field $\vec{E}(\mathbf{r})$ at the exciton position $\mathbf{r}$ generated by the environmental dipolar fluctuations (as illustrated in Fig. 1). This results in the interaction energy $H_{SB} = \vec{\mu} \cdot \vec{E}(\mathbf{r})$. For simplicity, we ignore the angular dependence in the following which only cause correction factors of the order of one [51]. Within the donor-acceptor model the exciton dipole moment is described by $\mu = |\vec{\mu}| = \mu_0 |i\rangle\langle i|$ where we furthermore have assumed that the dipole moments at each chromophore site

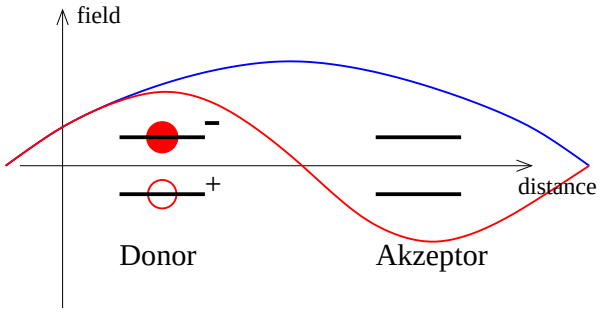


Figure 1. Donor and acceptor with two environmental field with different wave length are illustrated. The donor holds an electron in the excited state which forms with the hole left in the ground state an exciton having a finite electric dipole moment.

are the same (again neglecting factors of the order one due to angular dependencies). The electric field is proportional to the amplitude of the propagating normal modes of the medium, $E(\mathbf{r}) = \mathrm{sgn}\{\vec{E}(\mathbf{r})\} \cdot |\vec{E}(\mathbf{r})| = E_0(1/\sqrt{N}) \sum_{\mathbf{k}} q_{\mathbf{k}} e^{i\mathbf{kr}}$ finally leading to the interaction Hamiltonian in Eq. (2) with $\lambda_{\mathbf{k}}(\mathbf{r}) = (\mu_0 E_0/\sqrt{N}) e^{i\mathbf{kr}}$. Similar ideas have recently been used to understand the phonon influence on double quantum dot charge qubits [37, 38] or tunneling defects [51].

For propagating modes in three spatial dimensions the spectral function of intersite fluctuations between chromophores i and j becomes

$$J_{ij}(\omega) = \sum_{\mathbf{k}} \frac{\lambda_{\mathbf{k}}(\mathbf{r}_i)\lambda_{-\mathbf{k}}(\mathbf{r}_j)}{2\omega_{\mathbf{k}}} \delta(\omega - \omega_{\mathbf{k}}) = 2\alpha\omega e^{-\omega/\omega_c} \frac{\sin(\omega t_0)}{\omega t_0}$$
$$\text{with} \quad t_0 = \frac{r_{ij}}{v} \tag{9}$$

with the sound velocity v (assuming linear dispersion $\omega_{\mathbf{k}} = vk$ and $k = |\mathbf{k}|$), the distance $r_{ij} = |\mathbf{r}_i - \mathbf{r}_j|$ between site i and j, coupling strength α and upper cut-off ω_c using an exponential form for the cut-off function. For the small cut-off frequencies typical for biomolecular environments ($\omega_c \simeq \Delta$) the cut-off function will modify quantitatively but not qualitatively the results. However, no detailed information about the specific cut-off functions for biomolecular environments is available in the literature. The (on-site) spectrum is Ohmic (linear in ω) for the FMO complex [52, 23]. Linear dispersion for the normal modes is a strong assumption and it is not clear if the simple Debye picture holds in biological soft matter up to energies Δ. For on-site fluctuations at site i the spectral function simplifies

$$J_{ii}(\omega) = \sum_{\mathbf{k}} \frac{|\lambda_{\mathbf{k}}(\mathbf{r}_i)|^2}{2\omega_{\mathbf{k}}} \delta(\omega - \omega_{\mathbf{k}}) = 2\alpha\omega e^{-\omega/\omega_c} . \tag{10}$$

Alternatively one might consider localized environmental fluctuations with localization length ξ, which is taken to be independent of the mode energy ω, resulting in the spectral density

$$J_{ij}^{\mathrm{loc}}(\omega) = 2\alpha\omega e^{-\omega/\omega_c} e^{-r_{ij}/\xi} \tag{11}$$

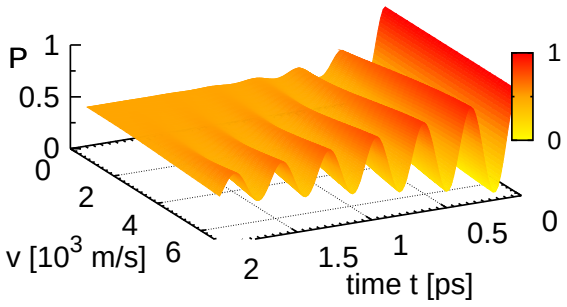


Figure 2. Occupation difference of donor and acceptor versus time and speed of sound for $\omega_c = \Delta = 106$ cm^{-1}, $T = 152$ K, $\alpha = 0.08$ and $r_{da} = 3.8$ Å assuming propagating environmental modes.

for the intersite spectrum whereas the on-site spectrum, Eq. (10), is unaltered.

The intersite spectrum $J_{ij}^{\rm loc}(\omega)$ vanishes for sites far apart $r_{ij} \gg \xi$ and the fluctuations at the donor and the acceptor sites are uncorrelated. The intersite spectrum becomes identical to the on-site spectrum for close sites $r_{ij} \ll \xi$. In the later case, the environmental fluctuations of both sites are fully correlated and thus actually identical. As illustrated in Fig. 1 by the blue line, both excitons then "see" the same electric field, which, in turn, only modifies the total energy but not the energy difference between donor and acceptor. Accordingly, these fully correlated fluctuations cannot influence the dynamics of the donor-acceptor system.

For the case of propagating modes, qualitatively the same holds. When $\Delta t_0 \gg 1$ all modes with $\omega \geq \Delta$ will not contribute to the intersite spectral function. At least at weak coupling ($\alpha \ll 1$), mainly the modes resonant with the tunneling splitting are relevant and thus we expect the intersite spectrum to be irrelevant. The environment acts as two independent baths at each chromophore site, as usually assumed in the literature. When the shortest wave length λ_c in the spectrum is larger than the distance between donor and acceptor, we have that $\omega_c t_0 = (r_{ij}/\lambda_c) \ll 1$. Then, the environmental fluctuations are fully correlated between the sites and thus do not affect the donor-acceptor system.

For the donor-acceptor system we can transform the Hamiltonian as discussed in Eq. (3) and then define a single effective spectral function (as for a spin-boson problem [20, 19]) resulting in

$$J_{\rm eff}(\omega) \;=\; 4\alpha\omega e^{-\omega/\omega_c}\left(1 - \frac{\sin(\omega t_0)}{\omega t_0}\right) . \tag{12}$$

In the limit $\omega_c t_0 \ll 1$, we get

$$J_{\rm eff}(\omega) \;\simeq\; 4\alpha t_0^2 \omega^3 e^{-\omega/\omega_c} \tag{13}$$

which is of super-Ohmic form. Super-Ohmic environmental fluctuations can neither cause overdamping (except at large temperatures) nor localization, in clear qualitative contrast to pure Ohmic fluctuations. This is a drastic qualitative effect which spatially correlated environmental fluctuations cause on coherent exciton transfer.

2.4. Dynamics of a single transfer step

Having determined the reduced density matrix by QUAPI, we can evaluate the occupation difference $P(t) = \langle \sigma_z \rangle$ between donor and acceptor. In Fig. 2, $P(t)$ is plotted over time versus sound velocity v with which the modes are assumed to propagate. We have chosen all parameter to match rather closely the properties of chromophores in the FMO complex [52]. We have used $\Delta = 106\ \mathrm{cm}^{-1}$ as tunneling element which corresponds to the largest coupling in the FMO complex [52] between chromophore 1 and 2 but have neglected the energy difference between the two sites. The distance between site 1 and 2 in the FMO complex of *Chlorobium tepidum* [7] is $r_{12} = 3.8$ Å which are the closest two chromophores. Site 2 and 7 are maximally apart, $r_{27} = 11.3$ Å. The bath cut-off frequency varies in the literature [52, 53] between $\omega_c = 32\ \mathrm{cm}^{-1}$ and $150\ \mathrm{cm}^{-1}$. To be specific, we choose $\omega_c = 106\ \mathrm{cm}^{-1}$ and temperature $T = 152$ K$= \Delta/k_B$.

We find that quantum coherent oscillations occur which decay within about 1 ps for the smallest value of the sound velocity of several hundred m/s. The environmental fluctuations are uncorrelated in this case. For larger sound velocities, meaning increasing correlations of the fluctuations, the decay slows down considerably as expected since the wave length of the modes causing decoherence becomes larger than the distance between the chromophores and thus cannot harm coherence any longer. We are not aware of experimental data regarding the precise values of sound velocities for the biological embedding materials of the FMO complexes. As a guide we might use the sound velocity of water, $v \simeq 1500$ m/s, which falls into the range of our plot. When frozen to ice, as in the low temperature experiments at 77 K or 180 K, one finds that $v \simeq 3150$ m/s and coherence lives considerably longer.

In order to elucidate the dependence of this effect on the system-bath coupling, Fig. 3 a) shows the result for $\alpha = 0.2$, resulting in a reorganization energy $\lambda \simeq 2\alpha\omega_c = 42.5\ \mathrm{cm}^{-1}$. This compares to the case shown in Fig. 2, where we have set $\alpha = 0.08$, resulting in a reorganization energy $\lambda \simeq 2\alpha\omega_c = 17\ \mathrm{cm}^{-1}$. The stronger coupling results in faster decoherence and the crossover to fully correlated environmental fluctuations causing long-time coherence is pushed to larger values of the sound velocity.

To address the temperature dependence, we show in Fig. 3 b) and c) the results for $P(t)$ for the same parameters as in Fig. 2, except that temperature is set to $T = 76$ K in b) and $T = 304$ K in c). At lower temperatures coherence expectedly survives longer whereas at higher temperatures coherence lives shorter. Nevertheless, for all temperatures the profound effect due to the finite sound velocity is present. This turnover between uncorrelated (strong decoherence) and strongly correlated (weak decoherence) environmental fluctuations thus is only weakly dependent on temperature. Next, we discuss the dependence of the crossover on the localization length ξ. Fig. 4 shows $P(t)$ for localized modes with localization lengths between 0 - 2 nm. Again as expected, for small localization lengths, the fluctuations at each site are uncorrelated and the occupation difference decays in less than a picosecond. Assuming a distance between donor and acceptor of $r_{12} = 3.8$ Å, the localization lengths plotted in

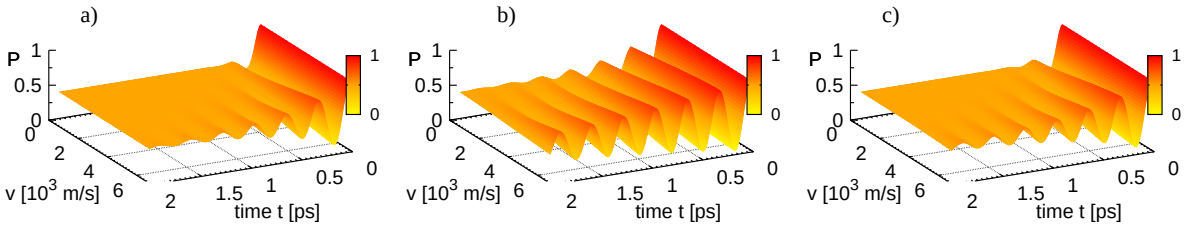


Figure 3. Occupation difference of donor and acceptor versus time and speed of sound assuming propagating environmental modes. Parameters are chosen to be $\omega_c = \Delta = 106$ cm^{-1} and $r_{da} = 3.8$ Å, and in a) $T = 152$ K, $\alpha = 0.2$, in b) $T = 76$ K, $\alpha = 0.08$, and in c) $T = 304$ K, $\alpha = 0.08$.

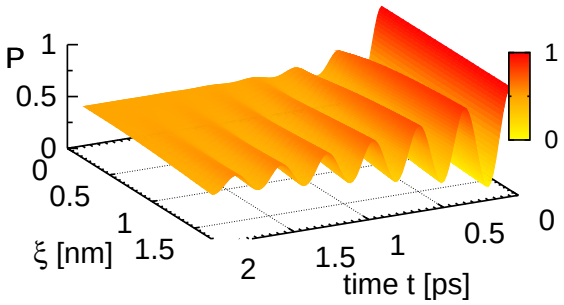


Figure 4. Occupation difference of donor and acceptor versus time and localization length ξ of localized environmental modes. Parameters are chosen as $\omega_c = \Delta = 106$ cm^{-1}, $T = 152$ K, $\alpha = 0.08$ and $r_{da} = 3.8$ Å.

Fig. 4, reach up to about four times the donor-acceptor distance. Then sizable correlations are expected and coherent oscillations for more than 2 picoseconds occur. In conclusion, assuming localized or propagating modes results qualitatively in the same behavior. The used parameters are all taken for the case of the FMO complex and thus our results strongly suggest that spatial correlations of the environmental fluctuations due to finite propagation time of the modes strongly influence the decay of coherence in exciton transfer processes. In order to judge on the quantitative effect, a comprehensive experimental investigation of the environmental modes is needed, in particular, whether the modes are propagating or localized, and accordingly, whether the sound velocity and/or the localization length is relevant. So far, we have discussed the influence of spatially correlated environmental fluctuations on the coherence of a *single* donor-acceptor pair. These results can in principle be extended to a chain of more chromophoric sites without changing the physical picture qualitatively.

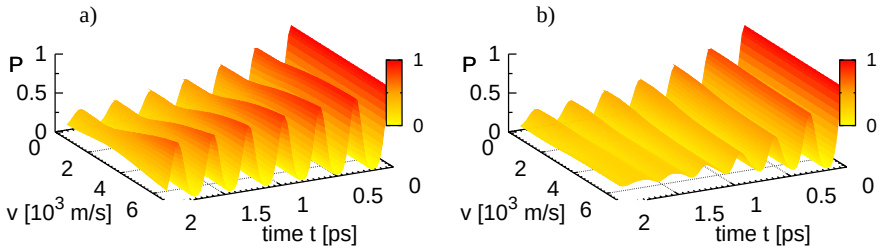


Figure 5. Probability $P_{d_1,d_2}(t)$ of both exciton being at the respective donor sites versus time and sound velocity assuming propagating environmental modes. Parameters are chosen to be $\omega_c = \Delta = 106$ cm^{-1}, $T = 15.2$ K, and $\alpha = 0.04$. The distances are for a) $r_{da} = 3.8$ Å and $r = 38$ Å , and for b) $r_{da} = 38$ Å and $r = 3.8$ Å.

3. Transfer in two chromophore pairs

3.1. Model

The FMO complex consists of three identical subunits, each of which consists of seven chromophoric sites and acts as a conductor for the excitons. Most likely, this structure has been optimized with respect to efficiency and seems to contain also some redundancy, which might be a measure of reliability in nature. In any case, the complex structure gives raise to the question whether a crosstalk between the subunits exists, and this even in a quantum coherent manner. In turn, the question whether this serves any purpose for functionality of increased efficiency is reasonable.

In order to approach this question on a qualitative level, simple low-dimensional effective models are necessary. We model a single subunit by one donor-acceptor pair and discuss in the following two such donor-acceptor pairs located at a distance r. We assume that each pair initially contains a single exciton at the respective donor site. We explicitly suppress exciton transfer from one pair to the other and start from the Hamiltonian

$$H_{\rm pda} = \frac{1}{2}\Delta \sum_{j=1}^{2} \{|d_j\rangle\langle a_j| + |a_j\rangle\langle d_j|\} + \sum_{j=1}^{2} \sum_{i=a_j/d_j} |i\rangle\langle i| \sum_{\mathbf{k}} \lambda_{\mathbf{k}}(\mathbf{r}_i) q_{\mathbf{k}} + \frac{1}{2}\sum_{\mathbf{k}} \left(p_{\mathbf{k}}^2 + \omega_{\mathbf{k}}^2 q_{\mathbf{k}}^2\right) . \quad (14)$$

We assume in the following that each chromophore couples separately to the environmental fluctuations but in contrast to the previous section, here there are two distinct distances involved. As before, each donor is separated by a distance $r_{da} = |\mathbf{r}_{a_1} - \mathbf{r}_{d_1}| = |\mathbf{r}_{a_2} - \mathbf{r}_{d_2}|$ from its acceptor. We assume this distance to be identical for both donor-acceptor pairs. The separation between both pairs is $r = |\mathbf{r}_{a_1} - \mathbf{r}_{a_2}| = |\mathbf{r}_{d_1} - \mathbf{r}_{d_2}|$.

3.2. Results

Since we have seen that propagating and localized (with a finite localization length) modes cause similar results for the decay of coherence, we restrict the following investigation to propagating modes. As before we set the tunneling element $\Delta = 106$ cm^{-1} and the fluctuation cut-off frequency $\omega_c = 106$ cm^{-1}. Fig. 5 shows the probability $P_{d_1,d_2}(t)$ that both excitons are located at the donor sites versus time for various values of the sound velocity for a weak coupling $\alpha = 0.04$. Note that we start from $P_{d_1,d_2}(t = 0) = 1$. The reorganization energy is then $\lambda \simeq 2\alpha\omega_c = 8.5$ cm^{-1} and a rather low temperature $T = 15.2$ K is chosen. In Fig. 5 a), we fix the distances $r_{da} = 3.8$ Å and $r = 38$ Å which reflects two rather distant donor-acceptor pairs. Both donor-acceptor pairs should thus be independent of each other since no direct coupling is assumed. We find a qualitatively similar behavior as for the case of a single pair as described in Section 2. Differences arise due to the weaker coupling and lower temperature. In contrast to the former case, we show the results for two close-by donor-acceptor pairs, $r = 3.8$ Å but with large donor-acceptor distance $r_{da} = 38$ Å in Fig. 5 b). Here, we find that the effect of decoherence increases with increasing sound velocity, in clear contrast to the previous discussion in Section 2. Hence, increasing spatial correlations between the two donor-acceptor pairs destroy quantum coherence.

For a quantitative investigation of this observation, we determine the associated decoherence rate Γ by fitting an exponentially damped cosine to the data for $P_{d_1,d_2}(t)$ shown in Fig. 5 and plot it in Fig. 6 versus the sound velocity for several distance ratios. As fundamental distance scale, we use $r_0 = 3.8$ Å, the distance of chromophore 1 and 2 in the FMO complex of *Chlorobium tepidum* [7]. At the sound velocity $v = 7600$ m/s, a mode can travel this distance within the time of $\Delta^{-1} = 50$ fs.

When both donor-acceptor pairs are far apart, $r = 10\, r_0$, and the distance between donor and acceptor is $r_{da} = r_0$ (shown by the blue up-triangle in Fig. 6), we recover the result of the previous Section 2. The decoherence rate decreases with increasing sound velocity. When the donor-acceptor distance is also large, $r_{da} = 10\, r_0$, there is no dependence of Γ on v for the investigated range of sound velocities (yellow left triangles in Fig. 6). The spatial correlations of the fluctuations simply do not extend from the donor to the acceptor site and thus the fluctuations are uncorrelated. When the two pairs are close to each other and the donor and acceptor sites are also close, the decoherence rate Γ decreases with increasing sound velocity (black circles in Fig. 6). A totally different case is reached when donor and acceptor sites are well separated, $r_{da} = 10\, r_0$ and $r_{da} = 100\, r_0$ (red squares and green diamonds in Fig. 6), but the two pairs are close, $r = r_0$. With increasing sound velocity, the decoherence rate increases and approximately doubles. The effect is slightly larger with larger distance between donor and acceptor.

With increasing sound velocity, the wave lengths of the propagating modes increase and thus spatial correlations of these modes reach further. When the fluctuations at the sites of both donor-acceptor pairs are fully correlated, which is approximately the

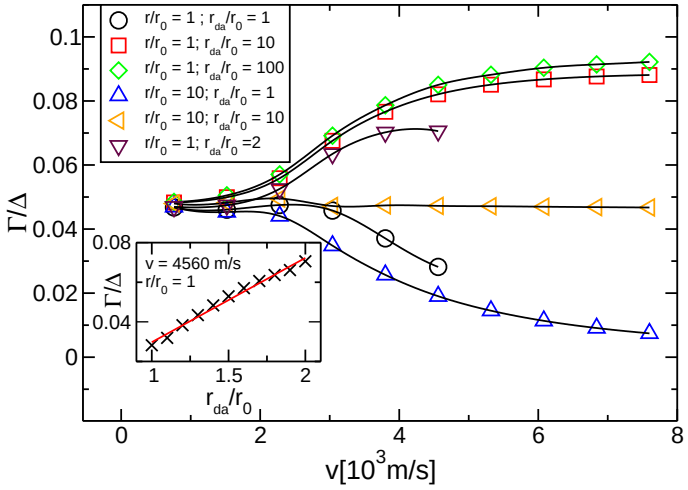


Figure 6. Decoherence rate Γ associated to the occupation probability $P_{d_1,d_2}(t)$ versus sound velocity v. Parameters are chosen as $\Delta = 106$ cm^{-1}, $T = 15.2$ K, $\alpha = 0.04$ and $\omega_c = 106$ cm^{-1}. Inset: Γ versus the ratio r_{da}/r_0 for $v = 4560$ m/s in the range $r_0 \leq r_{da} \leq 2r_0$.

case for sound velocities of $v \approx 7600$ m/s for $r = r_0$, then the fluctuations of the second donor (acceptor) equally influence the first one. Thus, the influence of the fluctuations effectively doubles which is reflected in doubling the decoherence rate. When donor and acceptors are closer, they as well become more correlated with increasing sound velocity, which, as discussed in the Section 2, results in decreasing decoherence rates. Thus, two effects are competing here. This also explains why for $r_{da} = 10\, r_0$ (red squares in Fig. 6) the increase of the rate Γ is weaker than for $r_{da} = 100\, r_0$ (green diamonds in Fig. 6). When both distances are equal, $r_{da} = r = r_0$ (black circles), the suppression of decoherence due to spatial correlations between donor and acceptor sites is the dominant effect, but it is weakened in comparison to the case of $r_{da} = r_0$ and $r_{da} = 10\, r_0$ (blue up triangles). Hence, we find two regimes, in which either one of the two effects dominates. How sharp the crossover between the two regimes is, becomes visible when looking at the data for $r_{da} = 2\, r_0$ and $r = r_0$. Here again, the decoherence rate Γ is increased by spatial correlations. Similar behavior (not shown) is also found for a smaller fluctuation cut-off frequency $\omega_c = 53$ cm^{-1} and otherwise identical parameters. The inset of Fig. 6 shows the change of the decoherence rate Γ when changing the donor-acceptor distance r_{da} from r_0 to $2\, r_0$ for a fixed sound velocity $v = 4560$ m/s. We find that in this regime, the change is linear in r_{da}.

Qualitatively the same happens for very large fluctuation cut-off frequencies $\omega_c = 1060$ cm^{-1} (as shown in Fig. 7a for otherwise identical parameters). Note that in this regime, non-Markovian effects are suppressed. The increase (decrease) of Γ for correlated donor-acceptor pairs (for correlated fluctuations at donor and acceptor site) becomes sharper. The influence of temperature is studied in Fig. 7b), which shows the decoherence rate Γ for a higher temperature, $T = 152$ K, but otherwise for the same

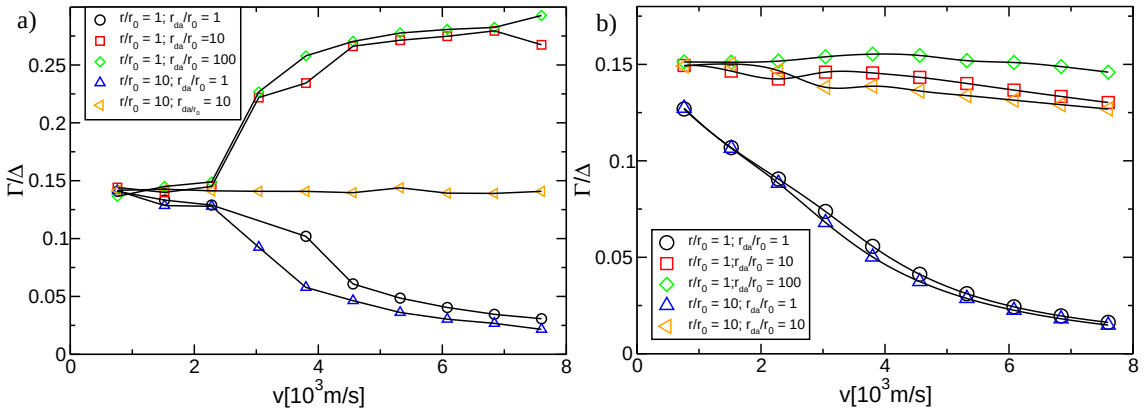


Figure 7. Decoherence rate Γ associated to the occupation probability $P_{d_1,d_2}(t)$ versus sound velocity v. Parameters are $\Delta = 106$ cm^{-1}, $\alpha = 0.04$, and in a) $T = 15.2$ K, $\omega_c = 1060$ cm^{-1}, and in b) $T = 152$ K, $\omega_c = 106$ cm^{-1}.

parameters as in Fig. 6. For small donor-acceptor distance, $r_{da} = r_0$, we find as before that the decoherence rate decreases with increasing sound velocity. However, the picture changes for large donor-acceptor distance, $r_{da} = 10r_0$. Then, the effect of decoherence is almost independent of the sound velocity, irrespective of the distance r between the donor-acceptor pairs.

4. Discussion and conclusions

To summarize, we have investigated the effect of spatially correlated environmental fluctuations on the quantum coherent transfer dynamics of excitons in donor-acceptor systems. Technically, spatially correlated environmental fluctuations can be included by adopting the numerical quasiadiabatic propagator path integral scheme. The fluctuations at each chromophore site generate a separate term in the Feynman-Vernon influence phase. The spatial correlations generate additional terms which then describe bath modes at different positions. Nevertheless, only the Feynman-Vernon influence phase is modified and the general QUAPI approach still remains feasible.

When the spatial correlations of the environmental fluctuations extend from the donor to the acceptor site, their decohering influence is strongly reduced since then, the energies at both sites are identically modified. The energy difference between donor and acceptor is not changed but only the global reference energy fluctuates which does not influence the dynamics. The spatial correlations of propagating modes are characterized by their wave length which itself is determined by the sound velocity assuming linear dispersion. In contrast, the spatial correlations of localized modes are determined by their localization length. Although these two cases are in principle different, the qualitative effect on quantum coherence is the same and depends only on the ratio of distance between donor and acceptor and the correlation length given either by the localization length or by the wave length of resonant modes.

Two donor-acceptor systems in close proximity in addition show an increase in the decoherence rate in dependence on their spatial distance. When the donor and acceptor sites are far apart and their fluctuations are only weakly correlated, correlations of close-by donor-acceptor pairs become relevant when the distance between the two donor-acceptor systems becomes small enough that their environmental fluctuations are correlated. Then, each donor-acceptor system "sees" the fluctuations at the site of the other one and thus the decoherence rate is doubled. For intermediate spatial distances, both effects are competing with each other. The effect of an increased decoherence rate, however, is suppressed at higher temperatures and is probably less relevant at room temperature.

Our results show that quantum coherence in the excitation transfer crucially depends on spatial correlations in the environmental fluctuations as soon as correlations lengths are of the order of the spatial distances of the chromophores. We have shown that for realistic material parameters (in particular, sound velocities), noticeable influence of the finite propagation times of environmental modes occurs. In fact, correlated fluctuations can reduce the decohering effect of the chromophore environment, when the correlation range extends over typical transfer distances within a chromophore chain. This effect even survives (even though diminished) up to room temperature and thus might be relevant for exciton transfer in biological systems. These findings are in line with the experimental findings [4, 9].

At the same time, correlations between different chromophore chains increase the decoherence rate and thus a close packing would be disadvantageous. This increase is, however, suppressed at room temperature. Thus, increased thermal fluctuations actually indirectly support quantum coherence since they reduce spatial correlations which would increase decoherence. This effect could be tested experimentally by performing the reported electronic coherence photon echo experiments at even lower temperature at a full FMO complex with all three subunits. At low temperature, spatial correlations between the FMO subunits should reduce quantum coherence more effectively than at higher temperatures.

Acknowledgments

This work was supported by the Excellence Initiative of the German Federal and State Governments.

References

[1] van Amerongen H, Valkunas L and van Grondelle R 2000 *Photosynthetic Excitons* (Singapore: World Scientific)

[2] Blankenship R E 2002 *Molecular Mechanisms of Photosynthesis* (London: World Scientific)

[3] Engel G S, Calhoun T R, Read E L, Ahn T K, Mancal T, Cheng Y C, Blankenship R E and Fleming G R 2007 *Nature* **446** 782

[4] Lee H, Cheng Y-C and Fleming G R 2007 *Science* **316** 1462

[5] Brixner T, Stenger J, Vaswani H, Cho M, Blankenship R E and Fleming G R 2005 *Nature* **434** 625

[6] Fenna R E and Matthews B W 1975 *Nature* **258** 573

[7] Li Y-F, Zhou W, Blankenship R E and Allen J P 1997 *J. Mol. Biol.* **271** 456

[8] van Groendelle R and Novoderezhkin V 2006 *Phys. Chem. Chem. Phys.* **8** 793

[9] Cheng Y C and Fleming G R 2009 *Annu. Rev. Phys. Chem.* **60** 241

[10] Collini E and Scholes G D 2009 *Science* **323** 369

[11] Mercer I P, El-Taha Y C, Kajumba N, Marangos J P, Tisch J W G, Gabrielsen M, Cogdell R J, Springate E and Turcu E 2009 *Phys. Rev. Lett.* **102** 057402

[12] Collini E, Wong C Y, Wilk K E, Curmi P M G, Brumer P and Scholes G D 2010 *Nature* **463** 644

[13] Calhoun T R, Ginsberg N S, Schlau-Cohen G S, Cheng Y C, Ballottari M, Bassi R and Fleming G R 2009 *J. Phys. Chem. B* **113** 16291

[14] Cao J S and Silbey R J 2009 *J. Phys. Chem. A* **113** 13825

[15] Herek J L, Wohlleben W, Cogdell R J, Zeidler D and Motzkus M 2002 *Nature* **417** 533

[16] Wohlleben W, Buckup T, Herek J L and Motzkus M 2005 *Chem. Phys. Chem.* **6** 850

[17] Savolainen J, Fanciulli R, Dijkhuizen N, Moore A L, Hauer J, Buckup T, Motzkus M and Herek J L 2008 *Proc. Natl. Acad. Sc.* **105** 7641

[18] Beljonne D, Curutchet C, Scholes G D and Silbey R J 2009 *J. Phys. Chem. B* **113** 6583

[19] Leggett A J, Chakravarty S, Dorsey A T, Fisher M P A, Garg A and Zwerger W 1987 *Rev. Mod. Phys.* **59** 1

[20] Weiss U 2008 *Quantum Dissipative Systems* 3rd edn (Singapore: World Scientific)

[21] Gilmore J B and McKenzie R H 2005 *J. Phys.: Condens. Matter* **17** 1735

[22] Gilmore J B and McKenzie R H 2006 *Chem. Phys. Lett.* **421** 266

[23] Gilmore J B and McKenzie R H 2008 *J. Phys. Chem. A* **112** 2162

[24] Förster T 1948 *Ann. Phys.* **437** 55; Förster T 1965 in *Modern Quantum Chemistry Part III* ed. O. Sinanoglu (New York: Academic 1965) pp. 93-137; May V and Kühn O 2004 *Charge and Energy Transfer Dynamics in Molecular Systems* (New York: Wiley-VCH)

[25] Mohseni M, Rebentrost P, Lloyd S and Aspuru-Guzik A 2008 *J. Chem. Phys.* **129** 174106; Rebentrost P, Mohseni M, Kassal I, Lloyd S and Aspuru-Guzik A 2009 *New J. Phys.* **11** 033003

[26] Rebentrost P, Mohseni M and Aspuru-Guzik A 2009 *J. Phys. Chem.* **B 113** 9942

[27] Rebentrost P, Chakraborty R and Aspuru-Guzik A 2009 *J. Chem. Phys.* **131** 184102

[28] Olaya-Castro A, Lee C F, Fassioli Olsen F and Johnson N F 2008 *Phys. Rev. B* **78** 085115

[29] Fassioli F, Nazir A and Olaya-Castro A 2009 preprint arXiv:0907.5183

[30] Fassioli F, Olaya-Castro A, Scheuring S, Sturgis J and Johnson N F 2009 *Biophys. J.* **97** 2464

[31] Plenio M B and Huelga S F 2008 *New J. Phys.* **10** 113019

[32] Caruso F, Chin A W, Datta A, Huelga S F and Plenio M B 2009 *J. Chem. Phys.* **131** 105106

[33] Caruso F, Chin A W, Datta A, Huelga S F and Plenio M 2009 preprint arXiv:0912.0122

[34] Rivas A, Huelga S F and Plenio M B 2009 preprint arXiv:0911.4270

[35] Chin A W, Datta A, Caruso F, Huelga S F and Plenio M B 2009 preprint arXiv:0910.4153

[36] Urboniene V, Vrublevskaja O, Trinkunas G, Gall A, Robert B and Valkunas L 2007 *Biophys. J.* **93** 2188

[37] Vorojtsov S, Mucciolo E R and Baranger H U 2005 *Phys. Rev. B* **71** 205322; Thorwart M, Eckel J and Mucciolo E R 2005 *Phys. Rev. B* **72** 235320

[38] Eckel J, Weiss S and Thorwart M 2006 *Eur. Phys. J. B* **53** 91

[39] Ishizaki A and Fleming G R 2009 *J. Chem. Phys.* **130** 234110; Ishizaki A and Fleming G R 2009 *J. Chem. Phys.* **130** 234111; Ishizaki A and Fleming G R 2009 *Proc. Natl. Acad. Sc.* **106** 17255

[40] Thorwart M, Eckel J, Reina J H, Nalbach P and Weiss S 2009 *Chem. Phys. Lett.* **478** 234

[41] Nalbach P and Thorwart M 2009 preprint arXiv:0911.5590.

[42] Eckel J, Reina J H and Thorwart M 2009 *New J. Phys.* **11** 085001

[43] Makri N 1995 *J. Math. Phys.* **36** 2430

[44] Thorwart M, Reimann P, Jung P and Fox R F 1998 *Chem. Phys.* **235** 61

[45] Thorwart M, Reimann P and Hänggi P 2000 *Phys. Rev. E* **62** 5808; Nalbach P and Thorwart M 2009 *Phys. Rev. Lett.* **103** 220401
[46] Scholak T, de Melo F, Wellens T, Mintert F and Buchleitner A 2009 preprint arXiv:0912.3560
[47] Palmieri B, Abramavicius D and Mukamel S 2010 *Phys. Chem. Chem. Phys.* **12** 108
[48] Palmieri B, Abramavicius D and Mukamel S 2009 *J. Chem. Phys.* **130** 204512
[49] Nazir A 2009 *Phys. Rev. Lett.* **103** 146404
[50] Lucke A, Mak C H, Egger R, Ankerhold J, Stockburger J and Grabert H 1997 *J. Chem. Phys.* **107** 8397
[51] Nalbach P, Terzidis O, Topp K A and Würger A 2001 *J. Phys.: Condens. Matter* **13** 1467
[52] Cho M, Vaswani H M, Brixner T, Stenger J and Fleming G R 2005 *J. Phys. Chem. B* **109** 10542
[53] Adolphs J and Renger T 2006 *Biophys. J.* **91** 2778